Supporting information

for Haunhorst and Hanschmann et al. 2013

Fig. S1 – Sequence alignment of Grx3 and Grx4 from various species

The alignment was produced using Clustal X. The thioredoxin (Trx) and monothiol glutaredoxin (Grx) domains are assigned below the sequences in blue and red, respectively. GLRX_DANRE, zebrafish Grx3; GLRX_HUMAN, human Grx3; GRX3_YEAST, *Saccharomyces cerevisiae* Grx3; GRX4_YEAST, *Saccharomyces cerevisiae* Grx4.

Fig. S2 – Lack of gross morphological changes in Grx3-depleted zebrafish

Apart from the reduced red blood cell count visible in the heart of embryos lacking Grx3 (arrows), no gross morphological changes could be detected in Grx3-depleted zebrafish (B) compared to control wildtype fish embryos (A) 48 hpf. scalebars, width = 0.3 mm.

Fig. S3 – Specificity of the Grx3 siRNA-induced phenotype in HeLa cells

To confirm the specificity of the siRNA used in this study (si-Grx3-1, blue in C), we compared different aspects of the depletion phenotype with that of HeLa cells transfected with the identical siRNA (si-Grx3-1*) from an alternative supplier (Ambion vs Eurogentec) as well as with a pool of four alternative siRNAs (si-Grx3-pool, red in C, supplier Dharmacon, accession numbers: J-019954-09,-10, -11, and -12). (A) Immunostaining of the indicated proteins extracted from HeLa cells transfected with scrambled control RNA (si-scr) or different siRNAs. (B) The activity of cytosolic aconitase normalized to lactate dehydrogenase activity was measured in samples of part A relative to the control cells.

Fig. S4 – Quality control of the subcellular fractionation procedure

Six days after the first transfection with siRNAs HeLa cells were permeabilized with digitonin, and the cell lysate was centrifuged for 10 min at 15,000 x *g* to obtain supernatant (cytosol) and pellet fractions (1). All fractions were analyzed by measuring the activities of (A) cytosolic lactate dehydrogenase (LDH) and (B) mitochondrial citrate synthase, two iron-independent marker

enzymes in order to monitor the efficiency of the subcellular fractionation procedure. The cytosolic fraction was virtually devoid of mitochondria. The pellet fraction, including enriched mitochondria, was essentially free of cytosolic proteins. All activities were normalized to those of control samples (scrambled siRNA, si-scr) of the respective compartment. 100% LDH activity corresponds to 4.55 ± 0.42 $U \cdot mg^{-1}$ of cytosolic protein, 100% citrate synthase activity to 1.13 ± 0.91 $U \cdot mg^{-1}$ of pellet protein (n = 5).

Fig. S5 – Grx3 depletion increases IRE binding activity of IRP1, but not that of IRP2

IRP binding activity of ^{32}P-labeled IRE of human ferritin mRNA was analyzed by RNA electrophoretic mobility shift assay (REMSA) and subsequent phosphorimaging according to (Leibold and Munro, 1988; Müllner *et al.*, 1989) with minor modifications. HeLa cells transfected either with scrambled siRNAs (si-scr) or with Grx3-specific siRNAs (si-Grx3) were harvested by trypsination, washed twice with PBS, and were snap-frozen in liquid nitrogen as cell pellets. Upon use, pellets were lysed in 'Munro buffer' (10 mM Hepes, pH 7.6; 3 mM $MgCl_2$; 40 mM KCl; 5% glycerol; 1 mM DTT; 1 mM PMSF; 0.2% NP40) (Leibold and Munro, 1988) and lysates were cleared by centrifugation. For the IRE-IRP binding reaction the cleared lysate samples corresponding to 1.8 µg protein were incubated with 125,000 cpm of a α-^{32}P[CTP]-labelled ferritin IRE-probe (Stehling et al., 2007). In order to induce maximal IRE-binding activity of IRP1, aliquots were pre-treated with 1.7% β-ME. IRE-binding of IRP2 was increased by addition of 0.3% β-ME according to a modification introduced by Zumbrennen *et al.* (2009) in order to improve the signal-to-noise ratio. Subsequently, RNAse T1 was added to degrade free IRE probes and stretches of IRP-bound probes which are not covered by the IRP proteins. Finally, reaction mixtures were mixed with sample buffer (30 mM Tris/HCl pH 7.5; 40% sucrose; 0.2% bromophenol blue; 125 µg heparin) in a 2:1 ratio. In some cases the sample buffer contained polyclonal rabbit anti-IRP1 or anti-IRP2 antiserum to allow separation of IRP1- and IRP2-bound IREs during native gel electrophoresis. Samples were loaded onto 8% polyacrylamide gels and separated at 10 V/cm for

2.5 hours using low concentrated TBE buffer (3.3 mM Tris, 3.3 mM borate, 0.66 mM EDTA). Gels were dried and subjected to autoradiography for three to four days. Positions of gel slots ('Start') and free probe fragments are indicated. **A)** Total IRP binding activity in the absence of β-mercaptoethanol (β-ME) was compared to the maximal binding activity induced by addition of 1.7% β-ME. Note that the increase in signal intensity is less pronounced in the si-grx3 sample than in the si-scr sample, consistent with the lowered IRP1 protein levels in Grx3-depleted cells. **B)** Pre-treatment of samples from part A with polyclonal anti-IRP2 (α-IRP2) antiserum induced formation of IRP2 immuno-complexes and allowed only IRP1 to enter the gel. The resulting radioactive signal corresponds to IRP1-bound IRE only. **C)** Pre-treatment of samples with polyclonal anti-IRP1 (α-IRP1) antiserum induced formation of IRP1 immuno-complexes and allowed only IRP2 to enter the gel. The autoradiographs show representative results for samples prepared six days after the first transfection with siRNA.

Leibold, E.A., and Munro, H.N. (1988). Cytoplasmic protein binds in vitro to a highly conserved sequence in the 5' untranslated region of ferritin heavy- and light-subunit mRNAs. Proc Natl Acad Sci U S A *85*, 2171-2175.

Müllner, E.W., Neupert, B., and Kühn, L.C. (1989). A specific mRNA binding factor regulates the iron-dependent stability of cytoplasmic transferrin receptor mRNA. Cell *58*, 373-382.

Stehling, O., Smith, P.M., Biederbick, A., Balk, J., Lill, R., and Mühlenhoff, U. (2007). Investigation of iron-sulfur protein maturation in eukaryotes. Methods Mol. Biol *372*, 325–342.

Zumbrennen, K.B., Wallander, M.L., Romney, S.J., and Leibold, E.A. (2009). Cysteine oxidation regulates the RNA-binding activity of iron regulatory protein 2. Mol Cell Biol *29*, 2219-2229.

Suppl. Figure 1

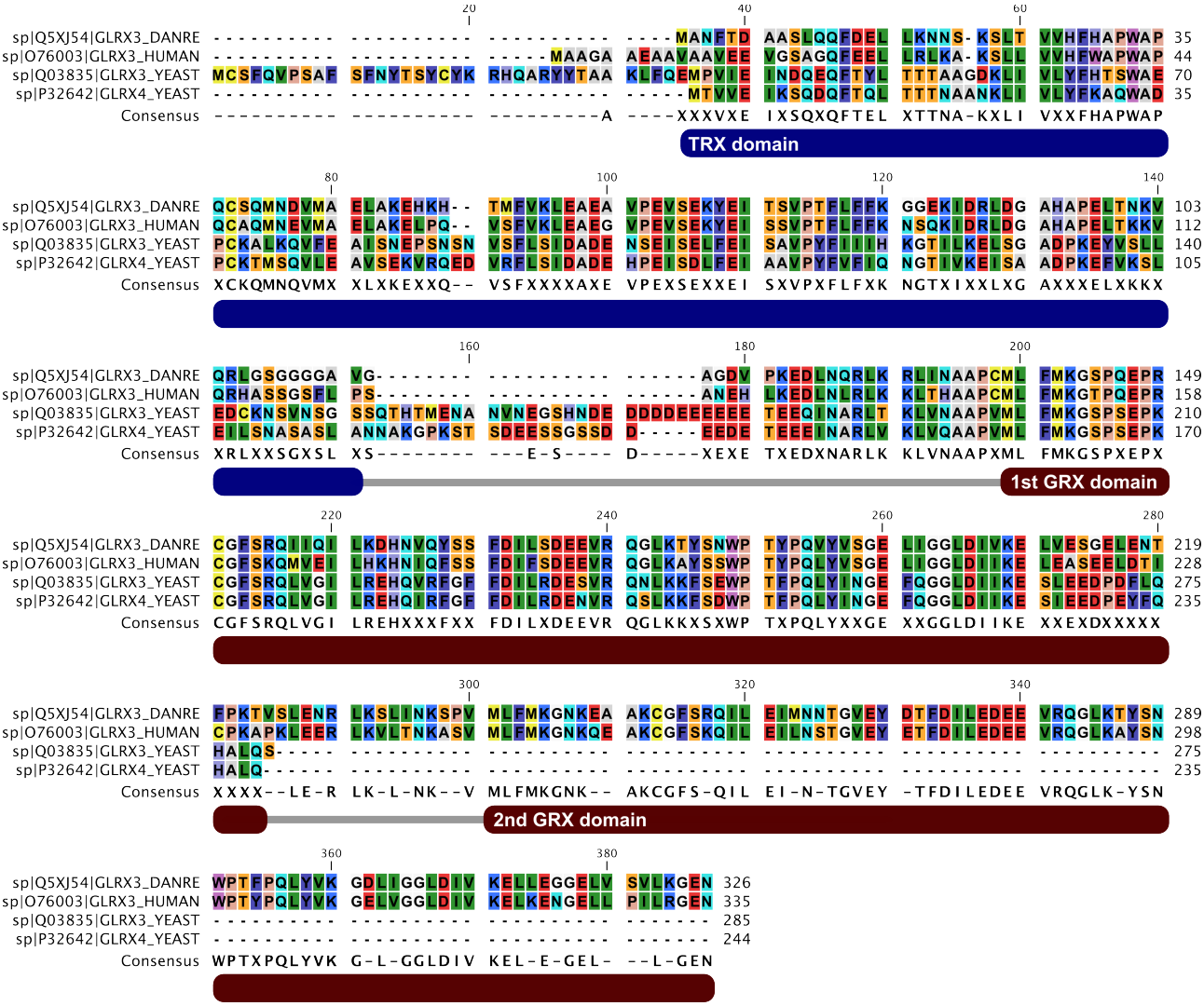

Suppl. Figure 2

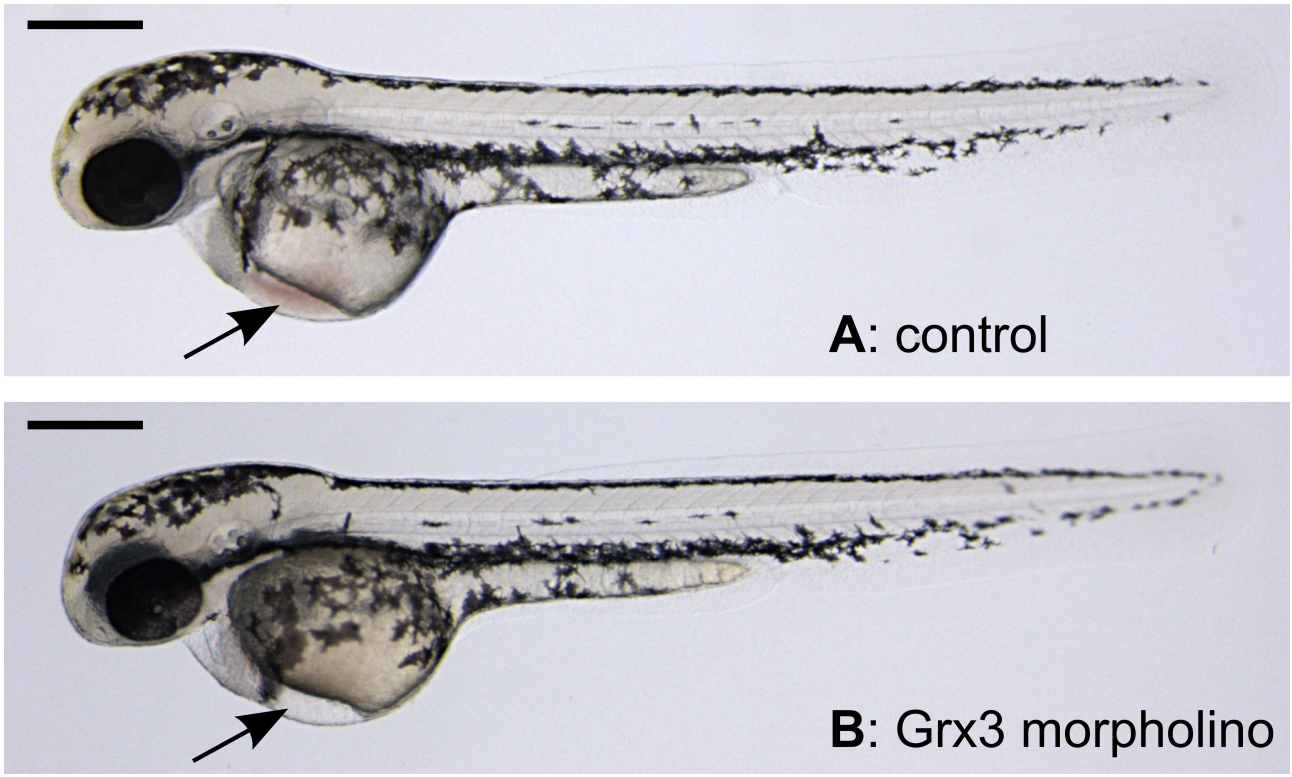

Suppl. Figure 3

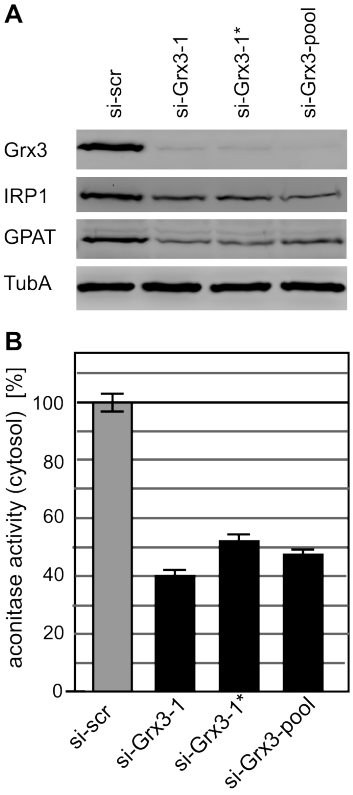

C

>huGLRX3 (hu_gi|13528998|gb|BC005289.1|)

GCTTCTGTCTGGCGGCGGCAGCATGGCGGCGGGGGCGGCTGAGGCAGCTGTAGCGGCCGTGGA
GGAGGTCGGCTCAGCCGGGCAGTTTGAGGAGCTGCTGCGCCTCAAAGCCAAGTCCCTCCTTGT
GGTCCATTTCTGGGCACCATGGGCTCCACAGTGTGCACAGATGAACGAAGTTATGGCAGAGTT
AGCTAAAGAACTCCCTCAAGTTTCATTTGTGAAGTTGGAAGCTGAAGGTGTTCCTGAAGTATC
TGAAAAATATGAAATTAGCTCTGTTCCCACTTTTCTGTTTTTCAAGAATTCTCAGAAAATCGA
CCGATTAGATGGTGCACATGCCCCAGAGTTGACCAAAAAAGTTCAGCGACATGCATCTAGTGG
CTCCTTCCTACCCAGCGCTAATGAACATCTTAAAGAAGATCTCAACCTTCGCTTGAAGAAATT
GACTCATGCTGCCCCCTGCATGCTGTTTATGAAAGGAACTCCTCAAGAACCACGCTGTGGTTT
CAGCAAGCAGATGGTGGAAATTCTTCACAAACATAATATTCAGTTTAGCAGTTTTGATATCTT
CTCAGATGAAGAGGTTCGACAGGGACTCAAAGCCTATTCCAGTTGGCCTACCTATCCTCAGCT
CTATGTTTCTGGAGAGCTCATAGGAGGACTTGATATAATTAAGGAGCTAGAAGCATCTGAAGA
ACTAGATACAATTTGTCCCAAAGCTCCCAAATTAGAGGAAAGGCTCAAAGTGCTGACAAATAA
AGCTTCTGTGATGCTCTTTATGAAAGGAAACAAACAGGAAGCAAAATGTGGATTCAGCAAACA
AATTCTGGAAATACTAAATAGTACTGGTGTTGAATATGAAACATTCGATATATTGGAGGATGA
AGAAGTTCGGCAAGGATTAAAAGCTTACTCAAATTGGCCAACATACCCTCAGCTGTATGTGAA
AGGGGAGCTGGTGGGAGGATTGGATATTGTGAAGGAACTGAAAGAAAATGGTGAATTGCTGCC
TATACTGAGAGGAGAAAATTAATAAATCTTAAACTTGGTGCCCAACTATTGTAAGAAATATTT
AATTACATTGGGAGCAGTTCATGATTTAGTCCTCAGAAATGGACTAGGAATAGAAAATTCCTG
CTTTCTCAGTTACATGTTTTGTGTATTTCACAATGTCGTGCTAAATAAATGTATGTTACATTT
TTTTCCCACCAAAAATAGAATGCAATAAACATCTTCAAATTATTAACGAAAAAAAAAAAAAAA
AAAAAAAAAAAAAA

siRNA-1
siRNA-pool

Suppl. Figure 4

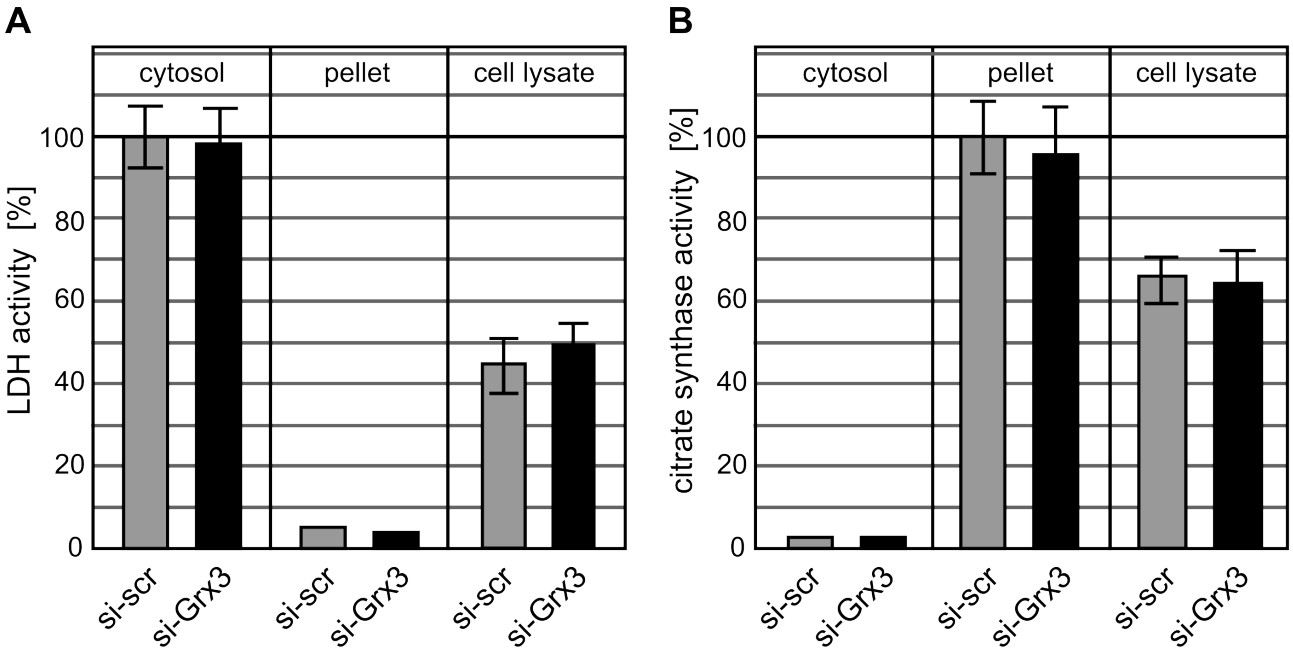

Suppl. Figure 5